SCIENTIFIC REP⚙RTS

# Moxifloxacin: Clinically compatible contrast agent for multiphoton imaging

Taejun Wang[1,*], Won Hyuk Jang[1,*], Seunghun Lee[2,*], Calvin J. Yoon[1,*], Jun Ho Lee[2], Bumju Kim[1], Sekyu Hwang[3], Chun-Pyo Hong[1], Yeoreum Yoon[2], Gilgu Lee[2], Viet-Hoan Le[1], Seoyeon Bok[1], G-One Ahn[1], Jaewook Lee[4], Yong Song Gho[4], Euiheon Chung[5], Sungjee Kim[3], Myoung Ho Jang[6], Seung-Jae Myung[7], Myoung Joon Kim[8], Peter T. C. So[9] & Ki Hean Kim[1,2]

Multiphoton microscopy (MPM) is a nonlinear fluorescence microscopic technique widely used for cellular imaging of thick tissues and live animals in biological studies. However, MPM application to human tissues is limited by weak endogenous fluorescence in tissue and cytotoxicity of exogenous probes. Herein, we describe the applications of moxifloxacin, an FDA-approved antibiotic, as a cell-labeling agent for MPM. Moxifloxacin has bright intrinsic multiphoton fluorescence, good tissue penetration and high intracellular concentration. MPM with moxifloxacin was demonstrated in various cell lines, and animal tissues of cornea, skin, small intestine and bladder. Clinical application is promising since imaging based on moxifloxacin labeling could be 10 times faster than imaging based on endogenous fluorescence.

Multiphoton microscopy (MPM) is a nonlinear fluorescence microscopic technique based on multiphoton (MP) excitation[1,2]. MPM is the technique of choice for fluorescence microscopy of thick tissue and live animals due to its high imaging depths and reduced photodamage compared to other fluorescence-based methods. MPM enables molecular imaging by using either exogenous markers or endogenous signals. Endogenous signals may be produced by autofluorescence (AF) or by other intrinsic nonlinear mechanism such as second harmonic generation (SHG) and third harmonic generation (THG). MPM has been applied to various biological studies including neurobiology[3,4], immunology[5], cancer biology[6], and pharmacology. MPM based on AF and other intrinsic contrasts have been used extensively as a label-free imaging method in pre-clinical or clinical research fields including dermatology[7–10], ophthalmology[10,11] and cancer biology[12–15]. However, AF signal is generally weak, thereby necessitating high excitation laser power or extension of pixel duration time[15,16]. We report the application of moxifloxacin as new contrast agent for *in vivo* cell-labeling in order to overcome the limitations of AF-based MP tissue imaging.

Moxifloxacin hydrochloride, hereafter referred to as moxifloxacin, is a fourth-generation fluoroquinolone antibiotic that prevents DNA replication of both Gram-positive and Gram-negative bacteria by inhibiting gyrase and topoisomerase IV activity[17]. Moxifloxacin is used in the clinic to treat or prevent a range of bacterial infections

[1]Division of Integrative Biosciences and Biotechnology, Pohang University of Science and Technology, 77 Cheongam-ro, Nam-gu, Pohang, Gyeongbuk 37673, Rep. of Korea. [2]Department of Mechanical Engineering, Pohang University of Science and Technology, 77 Cheongam-ro, Nam-gu, Pohang, Gyeongbuk 37673, Rep. of Korea. [3]Department of Chemistry, Pohang University of Science and Technology, 77 Cheongam-ro, Nam-gu, Pohang, Gyeongbuk 37673, Rep. of Korea. [4]Department of Life Sciences, Pohang University of Science and Technology, 77 Cheongam-ro, Nam-gu, Pohang, Gyeongbuk 37673, Rep. of Korea. [5]Department of Biomedical Science and Engineering, and School of Mechanical Engineering, Gwangju Institute of Science and Technology, 123 Cheomdan-gwagiro, Buk-gu, Gwangju 61005, Rep. of Korea. [6]Academy of Immunology and Microbiology, Institute for Basic Science, 77 Cheongam-ro, Nam-gu, Pohang, Gyeongbuk 37673, Rep. of Korea. [7]Department of Gastroenterology, University of Ulsan College of Medicine, Asan Medical Center, 88 Olympic-ro, 43-gil, Songpa-gu, Seoul 05505, Rep. of Korea. [8]Department of Ophthalmology, Asan University of Ulsan College of Medicine, Asan Medical Center, 88 Olympic-ro, 43-gil, Songpa-gu, Seoul 05505, Rep. of Korea. [9]Department of Mechanical Engineering and Biological Engineering, Massachusetts Institute of Technology, 77 Massachusetts Avenue, Cambridge, MA 02139, USA. *These authors contributed equally to this work. Correspondence and requests for materials should be addressed to K.H.K. (email: kiheankim@postech.ac.kr)
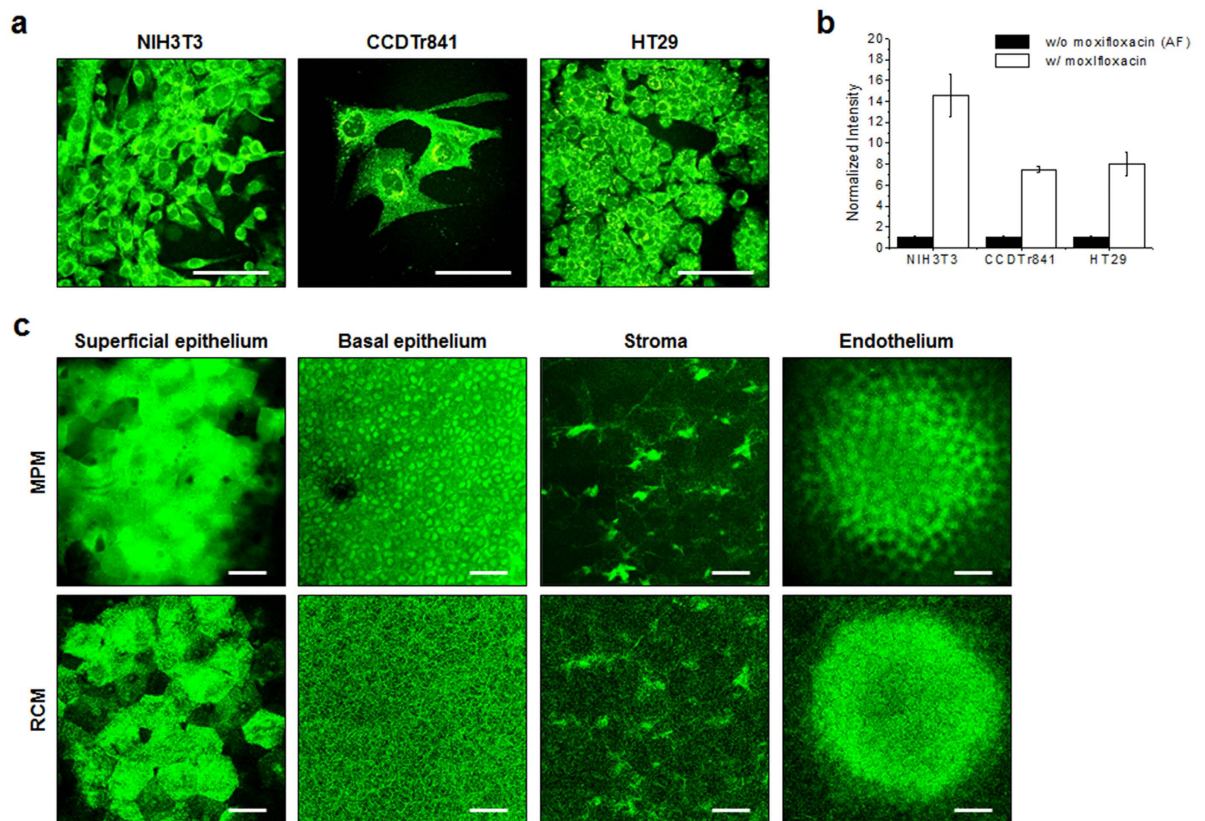
Figure 1. *In vitro* multiphoton microscopy (MPM) images of cell lines and intracellular moxifloxacin fluorescence intensities. MPM and reflectance confocal microscopy (RCM) images of a freshly extracted rat cornea. All MPM and RCM images are based on moxifloxacin fluorescence. (**a**) Cultured cell lines: mouse embryonic fibroblast (NIH3T3), human normal colon (CCDTr841), and human colon carcinoma (HT29). Representative MPM images of cell lines are presented as maximum intensity projection (MIP) images with a stepwise increment of $1\,\mu m$ in the z direction. Scale bars, $50\,\mu m$. (**b**) Quantification of intracellular moxifloxacin fluorescence intensities. Intracellular signal was enhanced significantly by approximately 10 times after moxifloxacin labeling. (**c**) MPM images of various layers of rat cornea comprising of superficial epithelium, basal epithelium, stroma, and endothelium. Corresponding RCM images of the same regions in the respective MPM images. Scale bars, $50\,\mu m$.

throughout the body, including the eye, skin, and respiratory tract, by topical, intravenous, and oral administration. Pharmacokinetic studies of moxifloxacin have shown good tissue penetration, high cellular-to-extracellular and tissue-to-serum concentration ratios compared to other fluoroquinolone antibiotics, attributed to its higher lipophilicity and aqueous solubility[18,19]. Moxifloxacin has intrinsic fluorescence with peak excitation and emission wavelengths at 290 nm and 500 nm, respectively, and its concentration in tissues is usually measured by high performance liquid chromatography (HPLC) of fluid extracts via fluorescence detection. Using moxifloxacin ophthalmic solution, we found that moxifloxacin can be readily excited via two-photon absorption at 700–800 nm[20] and has a high two-photon cross-section approximately 8 times smaller than that of fluorescein (pH 7.4) at 780 nm (Supplementary Fig. 1). MPM of moxifloxacin-treated mouse cornea showed the spatial distribution of moxifloxacin, where cells in the cornea were visible due to the high intracellular concentration of moxifloxacin, therefore yielding much stronger signal than AF contrast[20]. Intracellular concentration of moxifloxacin in human neutrophils and tissue-cultured epithelial cells was reported to be up to 10 times greater than that of the extracellular[21]. Therefore, these suggested the possibility of utilizing moxifloxacin as a nonspecific cell-labeling agent for MP tissue imaging in clinical applications. Here we demonstrate the applications of moxifloxacin as a nonspecific cell-labeling agent for MP imaging.

Results

To investigate the cellular labeling properties of moxifloxacin, we imaged by MPM a variety of *in vitro* cell lines of mice and human before and after treatment of $10\,\mu M$ moxifloxacin (Fig. 1a). Moxifloxacin-treated cell lines were detectable by approximately 7–14 times greater intracellular signal than that of AF at the same excitation laser power of 2.52 mW (Fig. 1b). In conjunction with the report that intracellular moxifloxacin concentration in cells is higher than that of the extracellular[21], we concluded that moxifloxacin is capable of cellular labeling and detection by MPM. We imaged a freshly extracted, moxifloxacin-treated rat cornea by both MPM and reflectance confocal microscopy (RCM), a standard method to examine the cornea at the cellular level (Supplementary Videos 1, 2).
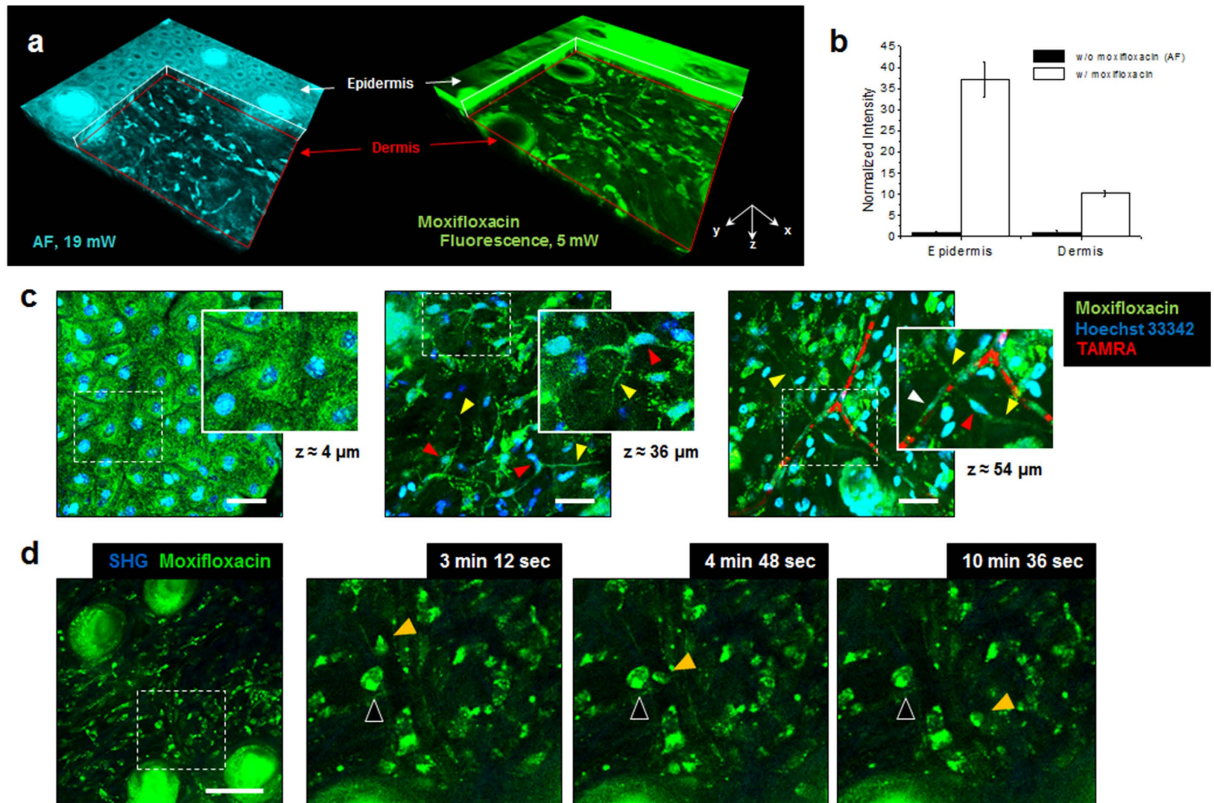
Figure 2. *In vivo* **MPM images of mouse hind limb skin.** (**a**) 3D rendered hind limb skin images based on autofluorescence (AF) and moxifloxacin fluorescence. Cellular structures in the dermis were captured by approximately 4 times higher laser power (19 mW) than that used for moxifloxacin-treated skin (5 mW). (**b**) Quantification of epidermis and dermis fluorescence intensities. The junction in between the epidermis and dermis was divided along the basal cell layer. (**c**) MPM hind limb skin images at different depths based on topically treated moxifloxacin (green), Hoechst 33342 (blue), and intravenously injected tetramethylrhodamine (TAMRA, red) for identification of cells, their nuclei, and blood vessels, respectively. The stratum spinosum is shown in the first MIP MPM image (2–6 μm). Thin fibrous structures (yellow arrowhead) branching from dermal cell bodies (red arrowhead) and capillary endothelial cells (white arrowhead) with blood vessel are shown in subsequent MIP MPM images (32–40 μm and 48–60 μm, respectively). Scale bars, 50 μm. (**d**) Mobile cell tracking in time-lapse imaging of the dermis after topical treatment of moxifloxacin, *in vivo*. Mobile cell (orange arrowhead) passing by a static cell (black arrowhead) is shown. Total elapsed imaging time is 25 min during anesthesia of the mouse. Scale bars, 50 μm.

In both, we were able to detect individual cells in the epithelium, stroma, and endothelium, confirming that moxifloxacin allowed for the visualization of cells by cellular labeling (Fig. 1c).

AF-based MPM provides cellular information of the skin down to the dermis at sufficiently high excitation laser powers[7,8,10]. To investigate moxifloxacin fluorescence-based MP imaging of skin *in vivo* using comparatively reduced excitation laser power, we first topically treated the skin of mouse hind limb with moxifloxacin (12.4 mM) after mild tape stripping to allow efficient delivery, then imaged with MPM and compared the results with AF-based MP imaging (Fig. 2a). While the layers of the epidermis were clearly visible by AF (Supplementary Video 3), the application of moxifloxacin significantly enhanced the visualization of cellular structures in the dermis, permitting the reduction of excitation laser power from 19 mW to 5 mW (Supplementary Fig. 2 and Supplementary Video 4). Fluorescence intensities from the epidermis and dermis were quantified under the same condition of constant excitation laser power of 5 mW along the z-axis (Fig. 2b). Fluorescence intensity, especially from the cellular structures in moxifloxacin-labeled dermis, was approximately 10 times higher than that of unlabeled dermis. In order to determine whether the signals captured in the dermis originated from intracellular moxifloxacin fluorescence, we counterstained with Hoechst 33342 (b2261, Sigma-Aldrich, Saint Louis, US) to locate nuclei within these structures. Additionally, to identify the vascular microstructures, we intravenously injected tetramethylrhodamine (TAMRA, D-7139, ThermoFisher Scientific, Waltham, US). Indeed, within each structure labeled by moxifloxacin, a nucleus was present, confirmed by spectral unmixing (Fig. 2c and Supplementary Figs 3 and 4). In the epidermis, cellular morphology and distribution of the cells of the stratum spinosum with their counterstained nuclei were visible. Below the epidermis, thin fibrous structures branching from cell bodies were visible. Based on morphology and location, these fibrous structures could possibly be nerves[22]. We also identified capillary endothelial cells by their narrow and elongated morphology running parallel with the TAMRA signal. Other cells in the dermis made visible by moxifloxacin could include
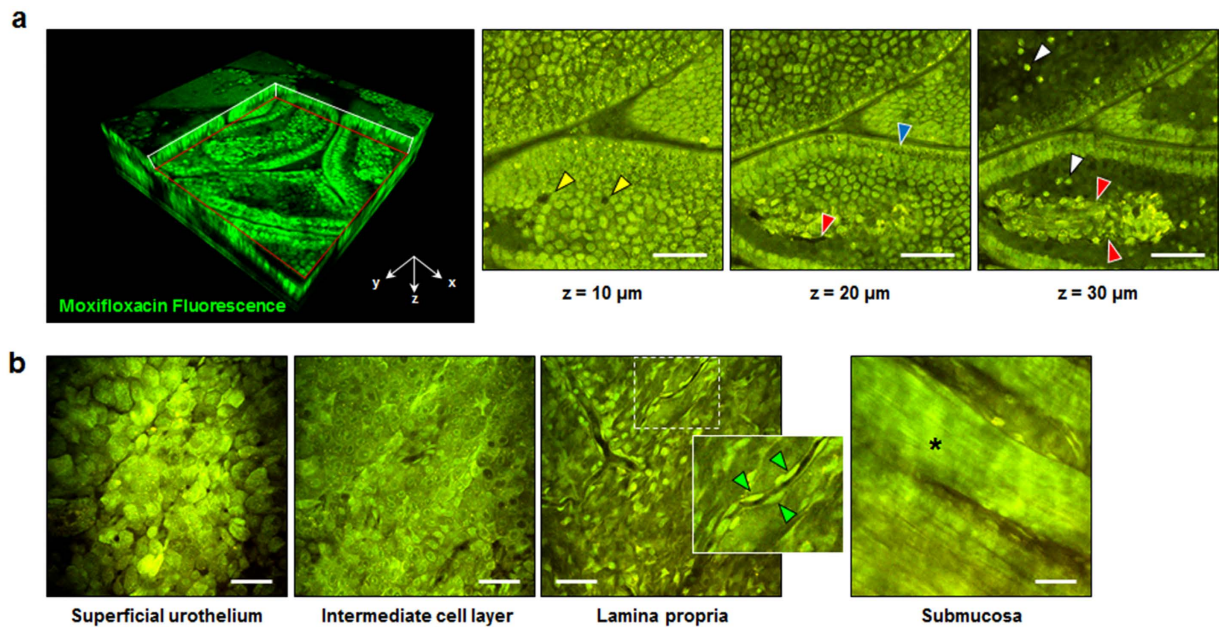
Figure 3. MPM images of freshly extracted mouse small intestine and rat bladder after topical treatment of moxifloxacin. (**a**) 3D rendered image of villus in small intestine (jejunum) and zoomed MPM images consisting of goblet cells (yellow arrowhead) and enterocytes (blue arrowhead) in epithelium, inner immune cells (white arrowhead), and capillaries (red arrowhead). Scale bars, $25\,\mu m$. (**b**) MPM images of rat bladder composed of structurally diverse layers such as the superficial urothelium ($z = 2\,\mu m$), dense intermediate cell layer ($z = 10\,\mu m$), lamina propria ($z = 32\,\mu m$) with capillary endothelial cells (green arrow), and submucosa ($z = 100\,\mu m$) consisting of muscle layer (black asterisk). Scale bars, $50\,\mu m$.

fibroblasts and immune cells. Moxifloxacin fluorescence-based MP imaging of isolated immune cells suggested that while neutrophils/monocytes, macrophages, eosinophils, and T cells could be visualized by moxifloxacin in the dermis (Supplementary Fig. 5), the identification of specific cells in the skin may be confirmed by usage of transgenic mice[23] or immunofluorescent labeling. Furthermore, we conducted time-lapse MP imaging, in which we observed dynamic movement of leukocytes within the dermis (Fig. 2d and Supplementary Video 5). Weak AF signal necessitates the extension of pixel duration time or the increase of incident laser power, which has been an obstacle for AF-based video-rate imaging and has also raised concerns of inducing thrombosis by two-photon excitation in *in vivo* skin samples. Therefore, we have conducted high-speed imaging on moxifloxacin-labeled and unlabeled mouse hind limb skin *in vivo* (Supplementary Fig. 6). Excitation laser powers of 31.2 mW and 51 mW were used for moxifloxacin-labeled and unlabeled dermis, respectively. Although AF-based skin imaging allowed for the monitoring of the dynamic cellular structures, extended imaging appeared to induce thrombosis due to high excitation power, as seen by the aggregation of endogenous fluorophores within the blood vessels in the dermis (Supplementary Video 6). In contrast, high-speed imaging of moxifloxacin-labeled dermis showed no signs of thrombosis and visualized more of the cellular microenvironment at 1.63 times reduced laser power (Supplementary Video 7).

Lastly, we briefly investigated labeling of freshly excised mouse small intestine and rat bladder by moxifloxacin. Moxifloxacin, as expected, effectively visualized cells in these tissues with a laser power in the range of 8 mW to 14 mW depending on the depth. In the moxifloxacin-labeled small intestine (jejunum), abundant cells within the villus (Fig. 3a and Supplementary Video 8), as well as enterocytes in the epithelial layer, can be clearly observed. Particularly, capillary structures were visible in the villus. Meanwhile in the rat bladder, the structurally diverse cell layers of the urothelium, lamina propria, and submucosa were clearly visualized with high contrast based on moxifloxacin fluorescence (Fig. 3b and Supplementary Video 9) suggesting the possible enablement of this approach as a real-time diagnostic tool for MP clinical endoscopy[24–26]. Additionally, endothelial cells outlining the capillaries in the lamina propria were observed.

Discussion

In this study, we demonstrated a novel MP tissue imaging method by using moxifloxacin, an FDA-approved compound, as a contrast agent for tissues such as cornea, skin, small intestine, and bladder. Moxifloxacin fluorescence-based MP imaging, even with 2 to 4 times reduced laser power than AF-based imaging, enabled effective and comparable visualization of various features of cells and their microenvironment, thereby allowing wide-field and high-speed imaging.

Optimized imaging parameters with short staining time and fast imaging speed are important for *in vivo* clinical imaging. Staining time may be dependent on the kinds of tissues and purpose of tissue studies. Staining time of less than approximately 20 minutes was enough for MP imaging of most tissues *in vivo*. On the other hand, imaging speeds should be at minimum 5–10 frames/s or preferably performed at video rates (>20 frames/s).

Faster imaging speed would be possible by adapting high-speed imaging methods. As such, other imaging parameters also have more room for improvement and, notwithstanding, experimental conditions for various human tissue imaging should be optimized in the future.

Limitations are still present in imaging human skin *in vivo* due to thicker and more folded characteristics compared to mouse skin. With an MPM imaging depth of less than 200 μm in the mouse skin, our current imaging depth will be an issue in the human skin. More careful optimization of imaging parameters is necessary for human skin imaging. Longer excitation wavelengths could be used to achieve an improved imaging depth, although it may reduce the advantage of moxifloxacin-based signal enhancement. In addition, usage of immersion materials for refractive index matching may help to reduce aberration and scattering of excitation light on the skin surface.

Because moxifloxacin is an antibiotic preventing DNA replication of both Gram-positive and Gram-negative bacteria, treatment of moxifloxacin for MP imaging may affect microflora. Therefore, moxifloxacin-based MPM may not be applicable to some research settings where undisturbed microflora is important. Notwithstanding, the negligible influence of moxifloxacin treatment on the investigation of cellular morphology in tissue strongly suggests the potential application of moxifloxacin as a nonspecific cell-labeling agent for MP clinical imaging.

Meanwhile, two-photon fluorescence lifetime imaging (FLIM) of tissue AF is a method used to detect metabolic changes of cells in tissue because fluorescence lifetime is highly sensitive to changes in cellular environment[27–29]. FLIM has been used in measuring oxidative stress[30] and detecting cancer cells. On the other hand, moxifloxacin used as a cell-labeling agent for signal enhancement in MP imaging may allow for high-speed imaging or imaging with relatively lower excitation power. However, moxifloxacin-based MP imaging does not provide any further information about cell functionality. Therefore, the combination of moxifloxacin-based MP imaging and AF-based metabolic MP imaging with fluorescence lifetime[30–34] will be useful. Because moxifloxacin fluorescence is stronger than AF, measurement of weak AF and fluorescence lifetime under the presence of moxifloxacin fluorescence will be difficult. However, since moxifloxacin concentration within cells will decrease over time, AF intensity and lifetime measurements before or a few hours after treatment will be possible.

Overall, we believe that moxifloxacin, an FDA-approved compound, is a promising contrast agent for MP clinical imaging due to sufficient intrinsic fluorescence and high intracellular concentration within tissue.

Methods

Moxifloxacin.   Moxifloxacin ophthalmic solution Vigamox (Alcon Laboratories, Fort Worth, US), was used to label various cell lines and cells in several tissues. This solution contains 0.5% (5 mg/mL) moxifloxacin hydrochloride (12.4 mM, pH 6.8) as the active ingredient. The moxifloxacin ophthalmic solution batch was always kept in its box to prevent possible photobleaching.

Multiphoton microscopy and data processing.   Multiphoton microscopy (MPM) with a Ti-Sapphire laser (Chameleon Vision II, Coherent) at 140 fs pulse width and 80 MHz pulse repetition rate was used (TCS SP5 II, Leica, Germany). 3D MPM imaging was performed with either of two 20× objective lenses (HCX APO L 20×, 1.0NA water immersion, Leica, Germany; XLUMPLFLN-20XW, 1.0NA, water immersion, Olympus, Japan) or a 25× objective lens (HCX IRAPO L 25×, 0.95NA, water immersion, Leica, Germany). Laser power was measured by a power meter (S310C, Thorlabs) and was accounted for beam clipping at the objective lens back pupil and transmittance across the objective lens. MPM images, composed of 512 × 512 pixels, were acquired and processed by LAS AF Lite (Leica, Germany) and MATLAB.

Cell preparation and imaging.   Dulbecco's Modified Eagle Medium (DMEM), Roswell Park Memorial Institute (RPMI) medium, fetal bovine serum (FBS), penicillin-streptomycin (PS), phosphate buffered saline (PBS), and trypsin-EDTA were purchased from Hyclone. HT29 human colon carcinoma and CCDTr841 human normal colon cells were obtained from Korean Cell Line Bank. HT29 cells were maintained in RPMI while CCDTr841 cells were maintained in DMEM, both supplemented with 10% (v/v) FBS and 1% (w/v) PS at 37 °C in a humidified atmosphere of 5% CO_2 in air. Cells were passaged when they reached approximately 80% confluence. Cells were seeded onto cell culture dish at a density of 1×10^5 cells and incubated overnight at 37 °C under 5% CO_2. Cells were treated with 10 μM of moxifloxacin for 1 hr before MP imaging. A 20× objective lens (XLUMPLFLN-20XW×, 1.0NA, water immersion, Olympus, Japan) was used for MPM. Prepared individual cell lines in culture dish were excited at 780 nm with an MP laser power of 2.52 mW. The emission light from moxifloxacin-treated cells was collected by 2 channels (blue: 300–430 nm; green: 430–680 nm). 3D volumetric scanning of cell lines in culture dish was performed at 0.08 frames/s and a stepwise increment of 1 μm in the z direction. MPM images of moxifloxacin-treated cell lines were processed as maximum intensity projection (MIP), and quantified as fluorescence intensities by using MIP images.

Animal preparation and ethical conduct.   Animal models were bred at the animal facility of POSTECH Biotech Center under specific pathogen-free (SPF) condition and had access to food and water *ad libitum*. All animal experimental procedures were conducted in accordance with institutional guidelines and regulations and approved by the Institutional Animal Care & Use Committee at POSTECH (2014-0073).

Rat cornea imaging.   Rat (Sprague-Dawley, male) was anesthetized via face mask administering a gas mixture of 1.5%/v isoflurane (Terrell™, Piramal) and medical grade oxygen, and was then sacrificed by cervical dislocation. An eye ball was extracted and mounted onto a custom-made acrylic eyeball holder. Images of cornea were acquired by MPM and reflectance confocal microscopy (RCM) based on topical treatment of moxifloxacin (12.4 mM) for 10 min of staining time. A 20× objective lens (HCX APO L 20×, 1.0NA water immersion, Leica, Germany) was used for both MPM and RCM. Excitation lasers were tuned to 780 nm and 633 nm for MPM and RCM, respectively. Laser power was approximately 12.15 mW at the ocular tissue for both MPM and RCM.

Emission light of moxifloxacin fluorescence-based MP imaging was collected by a single channel (green: 455–680 nm). Following, that of corneal cells from RCM was also taken into a single channel (green: 618–648 nm). 3D volumetric scanning of rat cornea was performed at 0.78 frames/s and a stepwise increment of 2 μm in the z direction.

Preparation for *in vivo* mouse hind limb skin imaging.   Mice (SKH1-HrHr, 6 weeks, female; BALB/c, 7 weeks, female) were anesthetized via face mask administering a gas mixture of 1.5%/vol isoflurane (Terrell™, Piramal) and medical grade oxygen. The mice were placed on a custom-made hind limb holder, which also functioned as a heating plate secured to a motorized x-y translational stage. Prior to imaging, fur was shaved when necessary, after which, mild tape stripping of the skin was performed approximately 10 times to remove the stratum corneum for efficient delivery of moxifloxacin.

Mouse hind limb skin imaging.   Excitation laser for AF-based imaging was tuned to 780 nm with a laser power held constant at 5 mW and 19 mW, for individual experiments, throughout the skin. Emission light was collected into 2 channels (blue: 300–430 nm; green: 430–680 nm). Following, moxifloxacin (12.4 mM) was topically applied to the tape stripped area and was left to diffuse for 30 min. Moxifloxacin was excited with 780 nm with a constant power of 5 mW throughout the skin. The emission light of moxifloxacin-based MP imaging was collected into the 2 aforementioned channels. 3D volumetric scanning was performed at 0.08 frames/s and stepwise increment of 2 μm in the z direction. For fluorescent labeling of cells and cell nuclei, 100 μL of a mixture of 5% (v/v) Hoechst 33342 (b2261, Sigma-Aldrich, Saint Louis, US) dissolved in moxifloxacin solution was treated for 30 min. To identify vascular structures, we intravenously injected 100 μL of 10 mg/mL tetramethylrhodamine (TAMRA, D-7139, ThermoFisher Scientific, Waltham, US) in PBS. Emission peaks of counterstained skin were furthest separated at 800 nm excitation, which allowed for maximum contrast with a laser power in the range of 8 mW to 21 mW depending on the depth. This emission light was collected into 4 channels (blue: 430–450 nm; green: 467–499 nm; yellow: 520–525 nm; red: 565–605 nm). 3D volumetric scanning of counterstained skin was performed at 0.25 frames/s with 2 lines averaging and a stepwise increment of 1.5 μm in the z direction.

Time-lapse imaging of hind limb skin.   To monitor the dynamic movement of cellular structures in moxifloxacin-labeled dermis, excitation laser was tuned to 780 nm for moxifloxacin fluorescence with a laser power of approximately 18.8 mW. The emission light of moxifloxacin fluorescence-based imaging was collected into 2 channels (blue: 300–490 nm; green: 490–680 nm). Imaging speed was 0.08 frames/s and total elapsed imaging time was 25 min during anesthesia of the mouse.

Antibodies.   All fluorescence-conjugated antibodies used for flow cytometric analysis were purchased from BD Biosciences and eBioscience. T cells were labeled with antibodies against TCRβ (H57-597) after FcR blocking with anti-CD16/CD32 antibodies (2.4G2). For eosinophil (MHC II⁻CCR3⁺) labeling, cells were stained with CD193 (83103). Neutrophils/monocytes (MHC II⁻CCR3⁻Gr1⁺CD11b⁺) were stained with Gr1 (RB6-8C5) and CD11b (M1/70). Macrophages (MHC II⁺F4/80⁺CD11b⁺) were stained with MHC II (M5/114.15.2) and F4/80 (BM8).

Isolation of immune cells and imaging.   For isolation of spleen macrophages, spleens were minced and digested in enzyme media (RPMI 1640 media containing 400 U/mL of collagenase D, 10 μg/mL DNase I, 3% FCS, 20 mM HEPES, 100 U/mL penicillin, 100 μg/mL streptomycin, 1 mM sodium pyruvate, and 1 mM NEAA) for 45 min at 37 °C. EDTA (final concentration of 10 mM) was added to the cell suspension and the cells were incubated for an additional 5 min at 37 °C. After filtering through a 100 μm cell strainer, the cells were spun in 17.5% Accudenz solution (Accurate Chemical & Scientific Co.) to enrich antigen presenting cells. Immune cells were purified by MoFlo Astrios cell sorter (Beckman Coulter). These isolated cells settled to the bottom of the Eppendorf tube and were labeled with moxifloxacin (12.4 mM) for 2 hr at 4 °C. Vortexed cell groups within moxifloxacin were moved onto well slide glass and sealed with a coverslip. A 20× objective lens (HCX APO L 20×, 1.0NA water immersion, Leica, Germany) was used for MPM. The excitation laser was tuned to 780 nm for moxifloxacin with a constant laser power of 3.6 mW. The emission light was collected into 4 channels (green: 430–480 nm; green: 500–550 nm; red: 565–605 nm; red: 625–675 nm). 3D volumetric scanning of isolated cells was performed at 0.78 frames/s with 2 lines averaging and a stepwise increment of 1 μm in the z direction. Representative MPM images of moxifloxacin-treated sorted cells were presented as MIP images (Supplementary Fig. 5). Intracellular and extracellular moxifloxacin concentrations were analyzed by boundary selection of single cells.

Mouse small intestine imaging.   To investigate the applicability of moxifloxacin for gut staining, fresh intact small intestine was surgically excised from wildtype mouse (BALB/c, 6 weeks, female) and was longitudinally cut to expose the villi of small intestine. The small intestine (jejunum) was labeled with moxifloxacin (12.4 mM) for 20 min and washed with PBS for 5 min. A prepared mouse small intestine, flattened with the villus side exposed, was mounted on glass slide and then covered with a coverslip. A 20× objective lens (HCX APO L 20×, 1.0NA, water immersion, Leica, Germany) was used for MPM. The excitation laser was tuned to 780 nm for moxifloxacin with a laser power in the range of 9.72 mW to 14.26 mW depending on the depth. The emission light was collected into 4 channels (green: 430–480 nm; green: 500–550 nm; red: 565–605 nm; red: 625–675 nm). 3D volumetric scanning was performed at 0.78 frames/s with 2 lines averaging and a stepwise increment of 2 μm in the z direction (from top of the villus to serosa).

Rat bladder imaging.   Rat (Sprague-Dawley, male) was anesthetized via face mask administering a gas mixture of 1.5%/v isoflurane (Terrell™, Piramal) and medical grade oxygen, and was then sacrificed by cervical

dislocation. The preparation of a fresh intact bladder tissue was the same as that of mouse small intestine. A 20× objective lens (XLUMPLFLN-20XW, 1.0NA, water immersion, Olympus, Japan) was used for MPM. The excitation laser was tuned to 780 nm for moxifloxacin excitation with a laser power in the range of 8.2 mW to 14.05 mW depending on the depth. The emission light was collected into 2 channels (green: 300–560 nm; red: 565–680 nm). 3D volumetric scanning was performed was the same as that of mouse small intestine (from urothelium to submucosa).

References

1. Denk, W., Strickler, J. H. & Webb, W. W. Two-photon laser scanning fluorescence microscopy. *Science* **248,** 73–76 (1990).
2. Zipfel, W. R. *et al.* Live tissue intrinsic emission microscopy using multiphoton-excited native fluorescence and second-harmonic generation. *Proc. Natl. Acad. Sci. USA* **100,** 7075–7080 (2003).
3. Svoboda, K. & Yasuda, R. Principles of two-photon excitation microscopy and its applications to neuroscience. *Neuron* **50,** 823–839 (2006).
4. Kerr, J. N. D. & Denk, W. Imaging *in vivo*: watching the brain in action. *Nat. Rev. Neurosci.* **9,** 195–205 (2008).
5. Germain, R. N., Miller, M. J., Dustin, M. L. & Nussenzweig, M. C. Dynamic imaging of the immune system: progress, pitfalls and promise. *Nat. Rev. Immunol.* **6,** 497–507 (2006).
6. Ellenbroek, S. I. J. & van Rheen, J. Imaging hallmarks of cancer in living mice. *Nat. Rev. Cancer* **14,** 406–418 (2014).
7. Cicchi, R., Kapsokalyvas, D. & Pavone, F. S. Clinical nonlinear laser imaging of human skin: a review. *Biomed. Res. Int.* **2014,** 1–14 (2014).
8. Tsai, T.-H., Jee, S.-H., Dong, C.-Y. & Lin, S.-J. Multiphoton microscopy in dermatological imaging. *J. Dermatol. Sci.* **56,** 1–8 (2009).
9. Quinn, K. P. *et al.* Diabetic wounds exhibit distinct microstructural and metabolic heterogeneity through label-free multiphoton microscopy. *J. Invest. Dermatol.* **136,** 342–344 (2016).
10. Wang, B.-G., König. K. & Halbhuber. K.-J. Two-photon microscopy of deep intravital tissues and its merits in clinical research. *J. Microsc.* **238,** 1–20 (2010).
11. Teng, S. W. *et al.* Multiphoton autofluorescence and second-harmonic generation imaging of the *ex vivo* porcine eye. *Invest. Ophthal. Vis. Sci.* **47,** 1216–1224 (2006).
12. Varone, A. *et al.* Endogenous two-photon fluorescence imaging elucidates metabolic changes related to enhanced glycolysis and glutamine consumption in precancerous epithelial tissues. *Can. Res.* **74,** 3067–3075 (2014).
13. Quinn, K. P. *et al.* Quantitative metabolic imaging using endogenous fluorescence to detect stem cell differentiation. *Sci. Reports* **3,** 1–10 (2013).
14. Levitt, J. M., McLaughlin-Drubin, M. E., Münger, K. & Georgakoudi, I. Automated biochemical, morphological, and organizational assessment of precancerous changes from endogenous two-photon fluorescence images. *PLoS One* **6,** e24765 (2011).
15. Thomas, G., van Voskuilen, J., Gerritsen, H. C. & Sterenborg, H. J. C. M. Advances and challenges in label-free nonlinear optical imaging using two-photon excitation fluorescence and second harmonic generation for cancer research. *J. Photochem. Photobiol. B: Biol.* **141,** 128–138 (2014).
16. Dela Cruz, J. M., McMullen, J. D., Williams, R. M. & Zipfel, W. R. Feasibility of using multiphoton excited tissue autofluorescence for *in vivo* human histopathology. *Biomed. Opt. Express* **1,** 1320–1330 (2010).
17. Drlica, K. & Zhoa, X. DNA gyrase, topoisomerase IV, and the 4-quinolones. *Microbiol. Mol. Biol. Rev.* **61,** 377–392 (1997).
18. Robertson, S. M. *et al.* Ocular pharmacokinetics of moxifloxacin after topical treatment of animals and humans. *Survey Ophthal.* **50,** S32–S45 (2005).
19. Wirtz, M. *et al.* Moxifloxacin penetration into human gastrointestinal tissues. *J. Antimicrob. Chemother.* **53,** 875–877 (2004).
20. Lee, S., *et al. In vivo* 3D measurement of moxifloxacin and gatifloxacin distributions in the mouse cornea using multiphoton microscopy. *Sci. Reports* **6,** 1–8 (2016).
21. Pascual, A., García, I., Ballesta, S. & Perea, E. J. Uptake and intracellular activity of moxifloxacin in human neutrophils and tissue-cultured epithelial cells. *Antimicrob. Agents Chemother.* **43,** 12–15 (1999).
22. Tschachler, E. *et al.* Sheet preparations expose the dermal nerve plexus of human skin and render the dermal nerve end organ accessible to extensive analysis. *J. Invest. Dermatol.* **122,** 177–182 (2004).
23. Li, J. L. *et al.* Intravital multiphoton imaging of immune responses in the mouse ear skin. *Nat. Prot.* **7,** 221–234 (2012).
24. König, K. *et al.* Clinical two-photon microendoscopy. *Microsc. Res. Tech.* **70,** 398–402 (2007).
25. Macaulay, C., Lane, P. & Richards-Kortum, R. *In vivo* pathology: microendoscopy as a new endoscopic imaging modality. *Gastrointest. Endosc. Clin. N. Am.* **14,** 595–620 (2004).
26. Wu, Y., Leng, Y., Xi, J. & Li, X. Scanning all-fiber-optic endomicroscopy system for 3D nonlinear optical imaging of biological tissues. *Opt. Express* **17,** 7907–7915 (2009).
27. Skala, M. C. *et al. In vivo* multiphoton microscopy of NADH and FAD redox states, fluorescence lifetimes, and cellular morphology in precancerous epithelia. *Proc. Natl. Acad. Sci. USA* **104,** 19494–19499 (2007).
28. Georgakoudi, I. & Quinn, K. P. Optical imaging using endogenous contrast to assess metabolic state. *Annu. Rev. Biomed. Eng.* **14,** 351–367 (2012).
29. Blacker, T. S. *et al.* Separating NADH and NADPH fluorescence in live cells and tissues using FLIM. *Nat. Comm*. **5,** 1–9 (2014).
30. Miura, Y. *et al.* Two-photon microscopy and fluorescence lifetime imaging of retinal pigment epithelial cells under oxidative stress. *Invest. Ophthalmol. Vis. Sci.* **54,** 3366–3377 (2013).
31. Dysli, C., Wolf, S. & Zinkernagel, M. S. Fluorescence lifetime imaging in retinal artery occlusion. *Invest. Ophthalmol. Vis. Sci.* **56,** 3329–3336 (2015).
32. Li, J. *et al.* Effect of recombinant interleukin-12 on murine skin regeneration and cell dynamics using *in vivo* multimodal microscopy. *Biomed. Opt. Express* **6,** 4277–4287 (2015).
33. Zhao, Y. *et al.* Longitudinal label-free tracking of cell death dynamics in living engineered human skin tissue with a multimodal microscope. *Biomed. Opt. Express* **5,** 3699–3716 (2014).
34. Stringari, C. *et al.* Metabolic trajectory of cellular differentiation in small intestine by phasor fluorescence lifetime microscopy of NADH. *Sci. Reports* **2,** 1–9 (2012).

Acknowledgements

Author Contributions

T.W. performed overall MP imaging experiments, processed data, and wrote the manuscript. W.H.J. and S.L. performed mouse hind limb skin imaging. C.J.Y. wrote the manuscript with T.W., checked cellular labeling of mouse hind limb skin using moxifloxacin and Hoechst 33342, and intravenously injected TAMRA with V.-H.L J.H.L. performed mouse and rat cornea imaging with S.L. B.K. helped with time-lapse imaging of mouse hind limb skin with W.H.J. S.H. and S.K. prepared cultured cell lines and cell-labeling protocol for cell lines. C.-P.H. and M.H.J. performed cell sorting from mice and helped with intracellular signal analysis. Y.Y. performed rat bladder imaging. G.L. performed data quantification with T.W. S.B. and G.-O.A. helped with discussion on immune cells in the skin. J.L. and Y.S.G. helped with discussion on cellular interactions and dynamics in the skin. E.C. provided various *in vivo* imaging protocols using animal models. S.M. and P.T.C.S. guided the experiments and revised the manuscript. M.J.K. prepared moxifloxacin solution and helped with corneal imaging. K.H.K. directed the overall project, analyzed experimental results and reviewed the manuscript with input from other authors.

Additional Information